

PAPER • OPEN ACCESS

Piezoelectric Energy Harvesting Based on Vertical Vibration of Car Body Induced by Road Surface Roughness

To cite this article: Hongyan Wang *et al* 2019 *IOP Conf. Ser.: Mater. Sci. Eng.* **470** 012036

View the [article online](#) for updates and enhancements.



IOP | ebooks™

Bringing you innovative digital publishing with leading voices to create your essential collection of books in STEM research.

Start exploring the collection - download the first chapter of every title for free.

Piezoelectric Energy Harvesting Based on Vertical Vibration of Car Body Induced by Road Surface Roughness

Hongyan Wang^{1,a}, Fengjuan Miao², Zhilong Sun¹ and Liqiu Jing¹

¹ College of Mechatronic Engineering, Qiqihar University, Qiqihar 161006, China

² College of Communications and Electronics Engineering, Qiqihar University, Qiqihar 161006, China

^a wanghongyan1993@163.com

Abstract. This paper presents the analysis of a cantilevered piezoelectric energy harvester (PEH) under the random vibration excitation of the car body. A two degree-of-freedom (2-DOF) quarter car model is established. The Matlab/Simulink simulation software is used to analyze the dynamic response of the car body under the random road excitation. The transient analysis of the PEH is carried out using ANSYS software to obtain the time-dependent voltage, current and power outputs of the PEH. The root mean square (RMS) power is used to evaluate the electricity generation of the PEH. The effect of the load resistance, the car speed, and the road surface roughness on RMS power are studied. The results show that it exists the optimal load resistance to achieve the maximum RMS power output for the vibration-based PEH. When the road surface roughness is constant, the increase of the car speed can induce the increase of the RMS power of the PEH. When the car speed is constant, higher RMS power outputs of the PEH can be achieved by increasing road surface roughness coefficient.

1. Introduction

With the rapid development of the low power electronic devices, the conventional batteries used to power these devices show some disadvantages, such as large volume, limited lifespan and high cost. Energy harvesting from ambient vibrations provides an exciting solution. Vibration energy can be converted into electricity via electrostatic mechanism [1], electromagnetic induction [2], or direct piezoelectric effect [3]. Among them, the PEHs have attracted more attention from researchers due to small volume, high power density, and easy to integrate with other electronics.

Among the literatures on piezoelectric energy harvesting, the input excitation is usually assumed to be a deterministic harmonic wave [4], while in practical situations, the mechanical excitation is a random signal. In this paper, the piezoelectric energy harvesting based on the vertical random vibration excitation of the car body is studied. Firstly, the dynamic responses of a 2-DOF quarter car under the road random excitation are obtained by using Matlab/Simulink simulation software. Subsequently, with the vertical displacement excitation from the car body, the time-dependent voltage, current and power outputs of the PEH are obtained by using ANSYS software. Furthermore, the effect of the load resistance, the car speed, and the road surface roughness on RMS power of PEH are investigated.

2. Modeling and simulation of road-car system



In this section, we establish the state-space equation for a 2-DOF quarter car model and use Matlab/Simulink simulation software to analyze the dynamic response of the car body under the random road excitation. The acceleration spectrum analysis of the car body provides a reference for the design of the PEH. The vertical displacement response of the car body is used as the excitation source of the PEH.

2.1. 2-DOF quarter-car model

Figure 1 shows a 2-DOF quarter car model. It comprises two moving masses (m_1 and m_2) connected in series with their respective springs (k_1 and k_2) and a damper (c) between m_1 and m_2 . m_1 and m_2 are the mass of the car wheel and the car body, respectively. k_1 and k_2 are the spring stiffness of the tyre and the suspension, respectively. c is the damping coefficient of the suspension. q is the excitation displacement of the road surface. u_1 and u_2 are the absolute displacement of m_1 and m_2 , respectively.

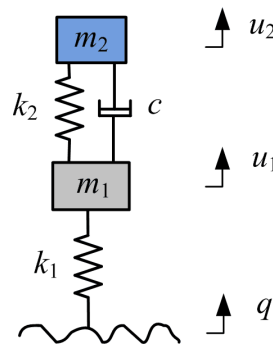


Figure 1. 2-DOF quarter car model.

The governing equations of the 2-DOF quarter car model can be written as

$$\begin{cases} m_2 \ddot{u}_2 + c(\dot{u}_2 - \dot{u}_1) + k_2(u_2 - u_1) = 0 \\ m_1 \ddot{u}_1 + c(\dot{u}_1 - \dot{u}_2) + k_2(u_1 - u_2) + k_1(u_1 - q) = 0 \end{cases} \quad (1)$$

where \dot{u}_1 and \dot{u}_2 are the velocities of the car wheel and car body in the vertical direction, respectively. \ddot{u}_1 and \ddot{u}_2 are the accelerations of the car wheel and car body in the vertical direction, respectively.

Defining the state space vector as

$$\mathbf{x} = [x_1 \ x_2 \ x_3 \ x_4]^T = [\dot{u}_2 \ u_2 \ \dot{u}_1 \ u_1]^T \quad (2)$$

$$\dot{\mathbf{x}} = [\dot{x}_1 \ \dot{x}_2 \ \dot{x}_3 \ \dot{x}_4]^T = [\ddot{u}_2 \ \dot{u}_2 \ \ddot{u}_1 \ \dot{u}_1]^T \quad (3)$$

$$\mathbf{y} = [y_1 \ y_2 \ y_3]^T = [\ddot{u}_2 \ \dot{u}_2 \ u_2]^T \quad (4)$$

$$\mathbf{u} = q \quad (5)$$

We can write the governing equations of the 2-DOF quarter car model in the state space form as

$$\begin{aligned} \dot{\mathbf{x}} &= \mathbf{A}\mathbf{x} + \mathbf{B}\mathbf{u} \\ \mathbf{y} &= \mathbf{C}\mathbf{x} + \mathbf{D}\mathbf{u} \end{aligned} \quad (6)$$

where

$$A = \begin{bmatrix} -\frac{c}{m_2} & -\frac{k_2}{m_2} & \frac{c}{m_2} & \frac{k_2}{m_2} \\ 1 & 0 & 0 & 0 \\ \frac{c}{m_1} & \frac{k_2}{m_1} & -\frac{c}{m_1} & -\frac{k_1+k_2}{m_1} \\ 0 & 0 & 1 & 0 \end{bmatrix}, \quad B = \begin{bmatrix} 0 \\ 0 \\ \frac{k_1}{m_1} \\ 0 \end{bmatrix}, \quad C = \begin{bmatrix} -\frac{c}{m_2} & -\frac{k_2}{m_2} & \frac{c}{m_2} & \frac{k_2}{m_2} \\ 1 & 0 & 0 & 0 \\ 0 & 1 & 0 & 0 \end{bmatrix}, \quad D = \begin{bmatrix} 0 \\ 0 \\ 0 \end{bmatrix}$$

A time-domain expression of the road surface roughness [5] is employed in this paper, which is written as

$$\dot{q} = 0.111[-vq + 40\sqrt{G_q}vw_0] \tag{7}$$

where \dot{q} is the excitation velocity of the road surface. v is the car velocity. w_0 is the white noise with the covariance value of $1m^2/s$. G_q is the road surface roughness coefficient. The road surface coefficient G_q is classified into eight levels, e.g., A, B, C, D, E, F, G, H, which have corresponding geometrical mean value as 16, 64, 256, 1024, 4096, 16384, 65536, and 262144, respectively. The unit of G_q is $10^{-6}m^3$.

2.2. *Vibration simulation of road-car model using Matlab/Simulink software*

The theoretical equations in section 2.1 are modeled in Matlab/Simulink, as shown in figure 2. This model includes mainly two modules, e.g., the input excitation module (equation (7)) and the 2-DOF quarter car module (equation (6)). The workspace is used to store the analytical results.

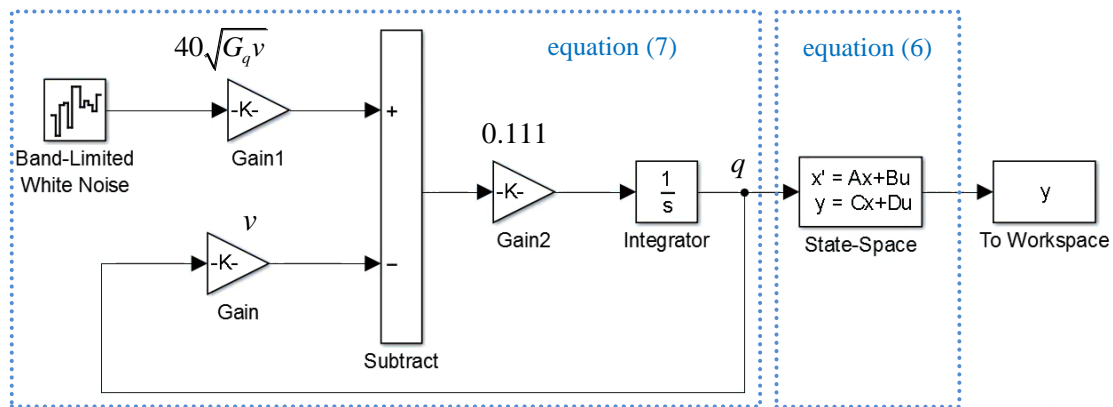


Figure 2. Simulink model for road-car system.

The parameters used in the dynamic analysis of the road-car system are $m_1=45.4$ kg, $k_1=192000$ N/m, $m_2=317.5$ kg, $k_2=22000$ N/m, $c=1520$ Ns/m, $v=10$ m/s, and $G_q=16 \times 10^{-6} m^3$ (Level A road surface). Figures 3(a), 3(b), and 3(c) show the vertical displacement, velocity and acceleration responses of the car body, respectively. The response time is 10 s. It can be seen from figures 3(a), 3(b), and 3(c) that the time-dependent displacement, velocity and acceleration responses are random. Figure 3(d) plots the acceleration power spectral density (PSD) of the car body. It can be seen from figure 3(d) that the acceleration PSD of the car body shows the highest peak at 1.074 Hz and the second highest peak at 11.23 Hz. The two peaks are induced by the resonance of the 2-DOF quarter car system. It is well known that the PEH is efficient near resonance. In this paper, we consider to design the PEH with the natural frequency near to 11.23 Hz to harvest vibration energy from the car body. We do not design the harvester with the natural frequency near to 1.074 Hz. The reason is that the fatigue cracking problem is easier to arise in the harvester with lower natural frequency (1.074 Hz) due to the larger amplitude of oscillation.

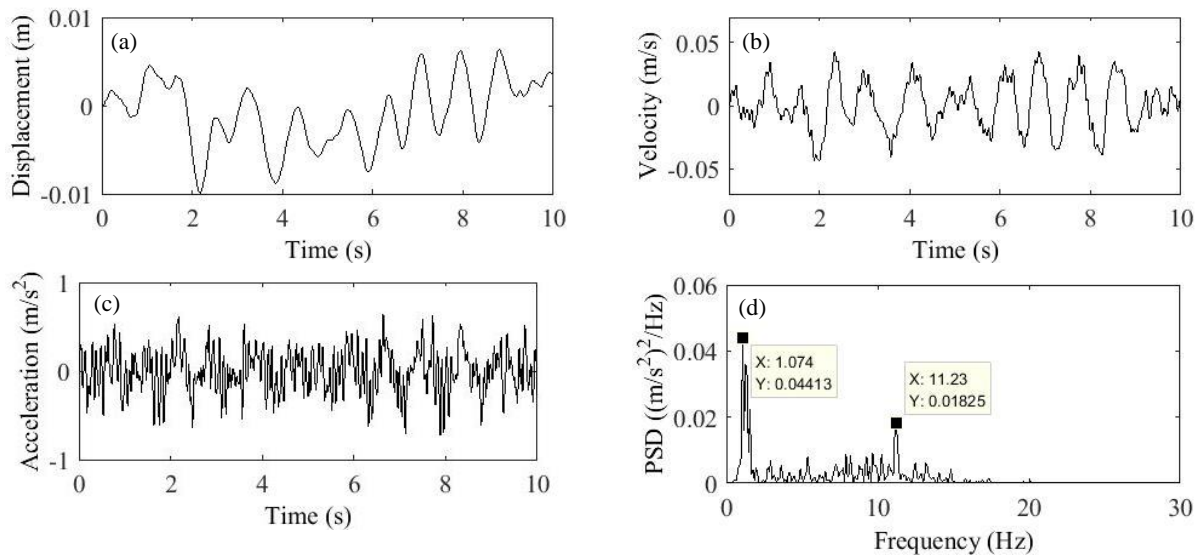


Figure 3. Dynamic responses of car body. (a) Time-dependent displacement; (b) Time-dependent velocity; (c) Time-dependent acceleration; (d) Acceleration power spectral density.

3. Vibration energy harvesting using cantilevered PEH

3.1. Model of cantilevered PEH

Figure 4 shows the structure of the cantilevered PEH. The beam is a piezoelectric sandwich structure with a central brass plate and two piezoelectric plates. The two piezoelectric plates were bonded to the top and bottom of the brass plate, respectively. The piezoelectric bimorphs are oppositely polarized in the z direction and are connected in series. The output terminal is directly connected to a resistor (R). L , w , h_p , and h_m are the beam length, the beam width, the thickness of piezoelectric plate, and the thickness of brass plate, respectively. M_t is the tip mass. The structural parameters used in the modeling of the PEH are $L=66$ mm, $w=20$ mm, $h_m=0.3$ mm, $h_p=0.2$ mm, and $M_t=0.09$ kg. The fundamental natural frequency of the PEH is 11.16 Hz, which is near to 11.23 Hz. Figure 5 shows the finite element (FE) model of the cantilevered PEH in ANSYS software. The 8-node hexahedral coupled-field element SOLID5 is used for the piezoelectric plates. The 8-node linear structural element SOLID45 is used for the brass plate. The circuit element CIRCU94 is used to model the resistor. The point element MASS21 is used for the lumped tip mass. The piezoelectric coefficients of PZT-5H used in ANSYS are available in literature [6]. The polarization direction of the piezoelectric material is represented by the sign of the piezoelectric constants. For the series-type piezoelectric bimorphs, the signs of the piezoelectric constants for the top and bottom piezoelectric plates are opposite. The electrode layer is simulated by coupling the nodal voltage DOF to ensure a uniform electrical potential. The mass-weighted damping and the stiffness-weighted damping are set as 1.3529 and 9.023e-6, respectively. The excitation source is from the vertical displacement of the car body.

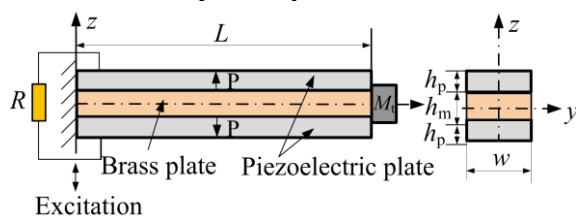


Figure 4. Structure of cantilevered PEH.

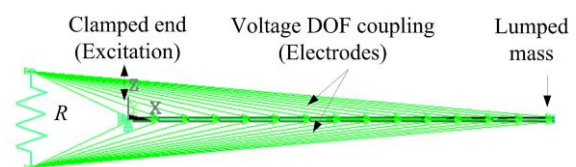


Figure 5. FE model of cantilevered PEH.

3.2. Electrical performance analysis of PEH

The transient analysis of the PEHs with various load resistance configurations are performed by using ANSYS software. Figures 6(a) , 6(c) and 6(e) show the time-dependent voltage, current and power for the PEH with the load resistance of 200 k Ω , respectively. Figures 6(b) , 6(d) and 6(f) show the time-dependent voltage, current and power for the PEH with the load resistance of 1000 k Ω , respectively. It is observed that the PEH with the load resistance of 1000 k Ω shows higher transient voltage outputs, lower transient current outputs, and lower transient power outputs (figure 6(b) , figure 6(d) and figure 6(f) as compared with those from the PEH with the load resistance of 200 k Ω (figure 6(a) , figure 6(c) and figure 6(e)). Figure 7 shows the variation in the power outputs of the PEH with the load resistance. In figure 7, the power outputs are the RMS values from the 10 s transient power. The power graph displays the peak value which corresponds to the optimal load resistance, $R=200$ k Ω .

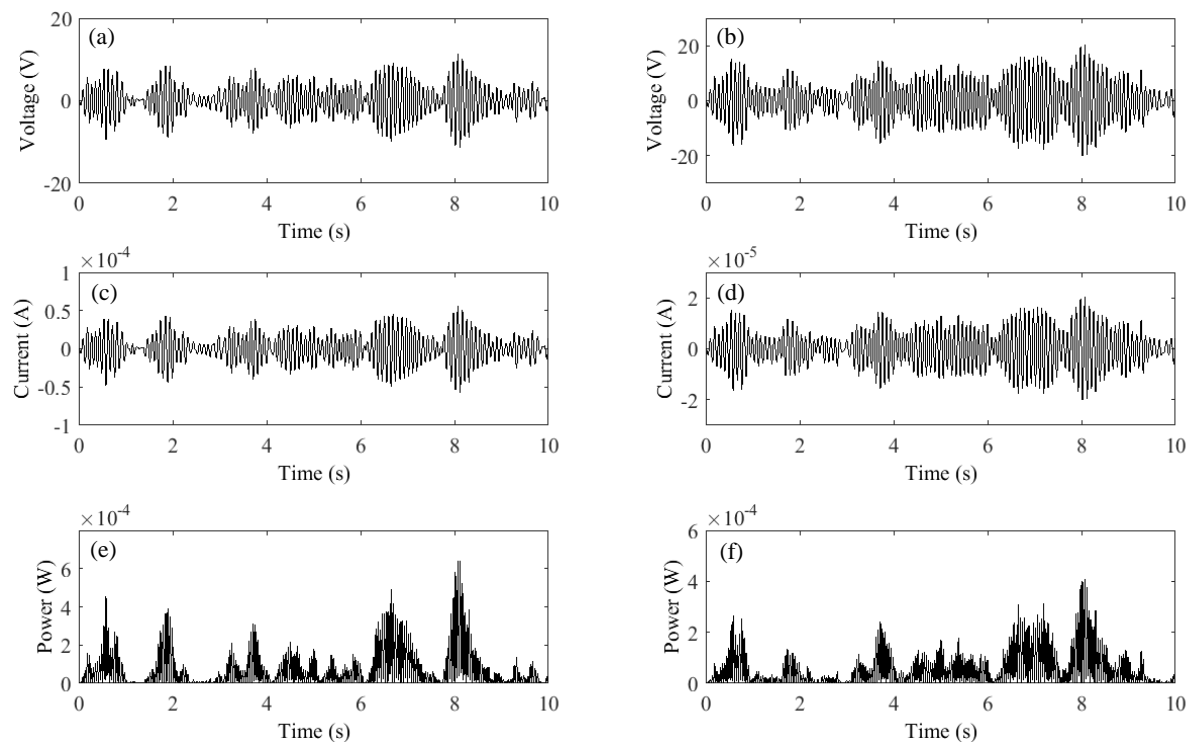


Figure 6. Voltage, current and power outputs of PEH. (a), (c) and (e) $R=200\text{k}\Omega$; (b), (d) and (f) $R=1000\text{k}\Omega$. Level A road surface. $v=10$ m/s.

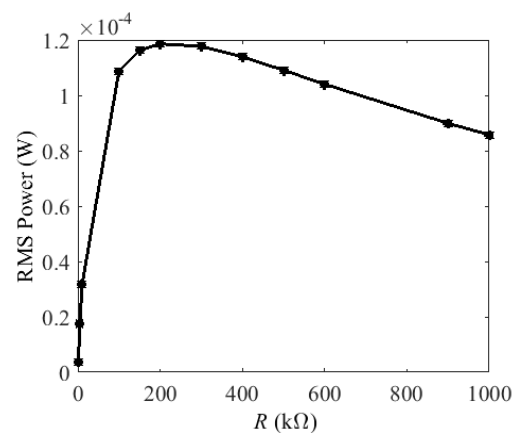


Figure 7. RMS power of PEH versus load resistance. Level A road surface. $v=10$ m/s.

3.3. Effect of vehicle speed and road roughness on power

With the optimal load resistance, we analyze the effect of car speed and road surface roughness on RMS power of the PEH. Figures 8(a) and 8(b) show the RMS power of the PEH for different car speed configurations and the road surface roughness configurations, respectively. It can be observed from figure 8(a) that with the same road surface roughness level, the increase of the car speed can induce the increase of the RMS power of the PEH. It can be observed from figure 8(b) that with the same car speed condition, the PEH can harvest higher RMS power when the road surface roughness becomes larger.

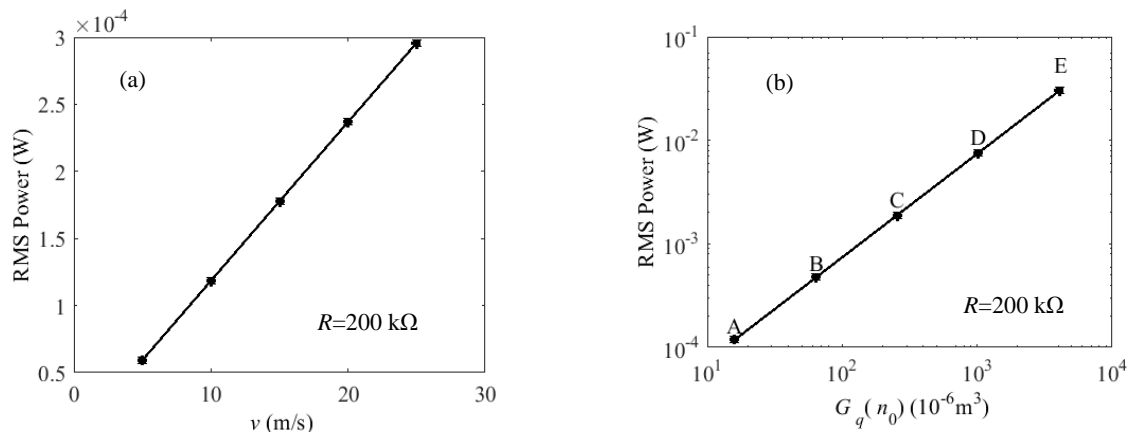


Figure 8. Effect of car speed and road surface roughness on RMS power of PEH. (a) Level A road surface; (b) $v=10\text{m/s}$.

4. Conclusions

In this paper, we analyze the dynamic response of the car body under the random road excitation. The vertical displacement of the car body is used as the excitation source for the electrical generation of the vibration-based PEH. The time-dependent voltage, current and power of the PEH are obtained by using the transient analysis in ANSYS software. The RMS power is used to evaluate the electricity generation of the PEH. We obtain the optimal load resistance of the PEH for the maximal power output of the PEH. With the optimal load resistance, the effect of the car speed and the road surface roughness on RMS power are studied. The results show that with the same road surface roughness, the increase of the car speed can induce the increase of the RMS power of the PEH. With the same car speed, larger road surface roughness coefficient can achieve higher RMS power of the PEH.

Acknowledgments

This work is supported by Heilongjiang Provincial Natural Science Foundation of China (No. LC2017028) and Fundamental Research Funds in Heilongjiang Provincial Universities of China (No.135209229).

References

- [1] Tao K, Wu J, Tang L, Hu L, Lye S W and Miao J 2017 *J. Micromech. Microeng.* **27** 044002
- [2] Samad F A, Karim M F, Paulose V and Ong L C 2016 *IEEE Sens. J.* **16** 1969-74
- [3] Fan K, Liu Z, Liu H, Wang L, Zhu Y and Yu B 2017 *Appl. Phys. Lett.* **110** 143902
- [4] Wang H and Tang L 2017 *Mech. Syst. Signal Pr.* **86** 29-39
- [5] Wu Z, Chen S, Yang L and Zhang B 2009 *Transactions of Beijing Institute of Technology* **29** 795-98
- [6] Wang H, Shan X and Xie T 2012 *J. Zhejiang Univ.-Sci A* **13** 526-37